HHS Public Access

Author manuscript

Part Part Syst Charact. Author manuscript; available in PMC 2017 August 04.

Published in final edited form as:

Part Part Syst Charact. 2016 June ; 33(6): 300–305. doi:10.1002/ppsc.201600032.

Mosaic Interdigitated Structure in Nanoparticle-Templated Phospholipid Bilayer Supports Partial Lipidation of Apolipoprotein A-I

Wangqiang Sun,

Department of Urology, Feinberg School of Medicine, Northwestern University, 303 East Chicago Avenue, Chicago, Illinois 60611, United States; School of Materials Science & Engineering, Hubei University of Technology, Wuhan 430068, China; Simpson Querrey Institute for BioNanotechnology, Northwestern University, 303 East Superior, Chicago, Illinois 60611, United States; Hubei Provincial Key Laboratory of Green Materials for Light Industry, Hubei University of Technology, Wuhan 430068, China

Dr. Weiqiang Wu,

Institute for Catalysis in Energy Processes and Center for Catalysis and Surface Science, Evanston, IL 60208, United States; Department of Chemistry, Northwestern University, Evanston, IL 60208, United States

Kaylin M. McMahon,

Department of Urology, Feinberg School of Medicine, Northwestern University, 303 East Chicago Avenue, Chicago, Illinois 60611, United States; Simpson Querrey Institute for BioNanotechnology, Northwestern University, 303 East Superior, Chicago, Illinois 60611, United States

Dr. Jonathan S. Rink, and

Department of Urology, Feinberg School of Medicine, Northwestern University, 303 East Chicago Avenue, Chicago, Illinois 60611, United States; Simpson Querrey Institute for BioNanotechnology, Northwestern University, 303 East Superior, Chicago, Illinois 60611, United States

Dr./Prof. C. Shad Thaxton

Department of Urology, Feinberg School of Medicine, Northwestern University, 303 East Chicago Avenue, Chicago, Illinois 60611, United States; Simpson Querrey Institute for BioNanotechnology, Northwestern University, 303 East Superior, Chicago, Illinois 60611, United States; International Institute for Nanotechnology, Northwestern University, Evanston, Illinois 60208, United States; Robert H. Lurie Comprehensive Cancer Center, Northwestern University, 303 East Superior, Chicago, Illinois 60611, United States

Graphical abstract

Correspondence to: Wangqiang Sun; C. Shad Thaxton.

Supporting Information

Supporting Information is available from the Wiley Online Library or from the author.

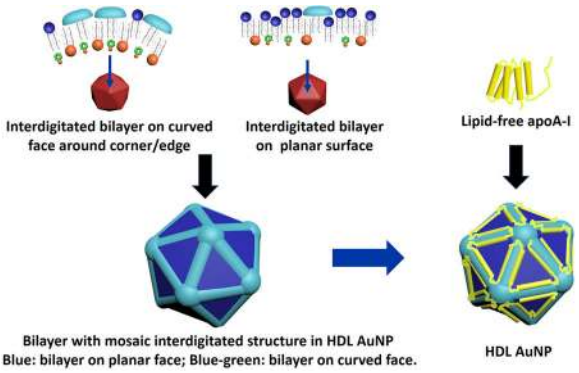

Using gold nanoparticle-templated high-density lipoprotein-like particles as a model, the nanoparticle-templated phospholipid bilayer is studied from the bottom-up. Data support the phospholipids have a mosaic interdigitated structure. The discontinuous lipid milieu supports partial lipidation of apolipoprotein A-I, different from an ordinary phospholipid bilayer, suggesting that synergy between nanoparticle templates and bound phospholipid layers can modulate amphiphilic proteins for desired functions.

Keywords

bio-nanostructure; lipidation; high-density lipoprotein; phospholipid; apolipoprotein A-I

Phospholipids prefer to form lamellar bilayer structures in aqueous media where diacyl chains are generally arranged tail-to-tail in a stacked arrangement.[1] Such phospholipid bilayers readily assemble and interact with a wide spectrum of proteins through strong lipid binding interactions, *i.e.* lipidation, which can further tailor the function of the proteins by adjusting their conformations.[2,3] Hence, phospholipid bilayers provide critical platforms for studying proteins. On the other hand, hybrid conjugates that combine phospholipid bilayers with nanostructures often exhibit new properties.[4] Certainly, a hallmark of many nanoparticle templates is their high surface area to volume ratio and resulting surface effects.[5] Thus, there is a strong synergy between nanoparticles and bound phospholipids, which may impact the phase structure of nanoparticle-templated phospholipids and induce new conformations and functions of lipidated proteins. Nevertheless, very little work has been reported in this area.

With a size ranging from 7 to 13 nm in diameter, high-density lipoproteins (HDLs) are dynamic natural nanoparticles that transport cholesterol in the systemic circulation.[3,6,7] As the principal protein of HDL, amphiphilic apolipoprotein A-I (apoA-I) scaffolds and remodels HDL particles by progressive lipidation, which significantly impacts a wide variety of diseases, including cardiovascular disease, cancer, and inflammation.[3,6,7] ApoA-I solubilizes phospholipid bilayers and adopts a continuous, fully lipidated, extended conformation (Figure 1a). This behavior provides a foundation for forming natural HDL particles.

Recently, we employed a gold nanoparticle (AuNP) as the template to assemble apoA-I with phospholipids to mimic HDLs (Figure 1b).[7] Compared to human HDLs, functional data

demonstrate the AuNP-templated HDL-like particles (HDL AuNPs) are robust acceptors of cellular cholesterol and may have therapeutic applications in diseases of cholesterol overload, lymphoma, and other indications.[7] In initial models of HDL AuNPs, the relationship between the AuNP and the bound phospholipids was poorly understood and we modeled the AuNP as an ideal sphere (Figure 1b).[7] The phospholipids on the surface of the HDL AuNP were modeled as an ordinary and uniform phospholipid bilayer that supports full apoA-I lipidation. However, functional data show that apoA-I on HDL AuNPs assumes a partly-lipidated conformation.[7d]

Motivated by these issues, we studied the structure of the nanoparticle-templated phospholipid bilayer, using HDL AuNP as a platform, from the bottom-up. For the first time, we report a mosaic interdigitated structure in the nanoparticle-templated phospholipid bilayer which supports partial lipidation of apoA-I. In this work, we first imaged the structure of bare AuNPs with transmission electron microscopy (TEM). Then we investigated HDL AuNPs layer by layer with X-ray photoelectron spectroscopy (XPS). Also we measured HDL AuNPs subjected to lipid extraction by UV-vis spectroscopy and scanning transmission electronic microscopy (STEM). Lastly, we detected the melting phase transition of acyl chains to explore structures of different phospholipid bilayers on AuNPs with *in-situ* diffuse reflectance infrared Fourier transform spectroscopy (DRIFTS). The results are summarized in a new model (Figure 1c). Data suggest that the AuNP is icosahedral, not an ideal sphere. Further, the phospholipid bilayer is not an ordinary bilayer, but a mosaic interdigitated bilayer, synergistically determined by the AuNP substrate and the molecular structure of the phospholipids. Finally, apoA-I assembles along borders between domains, close to the edges of the icosahedral AuNP, and decreases defects serving to improve bilayer stability. As such, apoA-I is constrained from achieving a fully extended conformation and remains partly lipidated.

Usually, most noble metals crystallize in a face-centered cubic (FCC) lattice, in which the (111) surface has the lowest surface energy.[8] In solution, twinned nuclei usually exhibit a higher population than single crystalline ones, which leads to the preferred formation of twinned nanoparticles.[8] Twinned nanoparticles can adopt morphologies with surfaces bounded only by {111} facets to accommodate the strain in the nanoparticles induced by the existence of twin defects.[8] When nanoparticles are small, multiply twinned particles (MTPs) minimize their surface energy by approaching a spherical shape, which is most effectively achieved with the icosahedron, the thermodynamically stable morphology.[8] In Figure 2a, the TEM image reflects the characteristic varying contrast of MTPs in the AuNPs we employed (80 nM, 5 ± 0.75 nm, in aqueous solution) to form HDL AuNPs.[9] Figure 2b further shows the high-resolution TEM (HRTEM) “fingerprints” of icosahedral particles.[9] Different to our original model, these data illustrate the bare AuNPs are icosahedrons, not ideal spheres.

An icosahedral AuNP is composed of 20 equally sized tetrahedral subunits of regular FCC (Figure 2c).[8] These tetrahedral subunits cannot completely fill the space of an icosahedron, which results in angular misfits. Thus, besides twin boundaries, there are many defects, such as stacking faults, dislocations, steps, and twist boundaries along the edges.[8] As such, the icosahedral AuNP consists of 20 separated planar faces surrounded by curved faces, with

defects, around 12 corners and 30 edges. Ultimately, the icosahedral AuNP has a mosaic surface.

In HDL AuNPs (Figure 1b), two different phospholipids are employed: 1,2-dipalmitoyl-sn-glycero-3-phosphoethanolamine-N-[3-(2-pyriidyldithio)propionate] (PDP PE), a disulfide-functionalized phospholipid, and 1,2-dipalmitoyl-sn-glycero-3-phosphocholine (DPPC), an ordinary phospholipid. Our original model hypothesized that these lipids combined to form an ordinary and uniform bilayer due to assumptions that AuNPs are spherical and the strong Au–S bond (~ 50 kcal/mol), PDP PE was assumed to self-assemble on the surface of AuNPs to form a supported thiolate self-assembled monolayer (SAM) like ordinary sulfur containing organic molecules.[10] Next, DPPC further assembled on the SAM to form the outer monolayer of a supported bilayer. Since AuNPs are not ideal spheres, we investigated the structure of bound phospholipids on their surfaces.

We first investigated the outer surface of HDL AuNPs by XPS, compared with pure DPPC, PDP PE and apoA-I (Supporting Information, Figure S1 and S2). The N 1s spectrum can be deconvoluted into three components (Figure 3a): 1) the peak at 402.58 eV mainly related to the unique protonated nitrogen in the choline of DPPC and alkaline residues in apoA-I, 2) the peak at 400.18 eV for the peptidic nitrogen in apoA-I and the weak amidic nitrogen in PDP PE, and 3) the peak at 399.18 eV uniquely assigned to the pyridinic nitrogen in PDP PE.[11] Further, the C 1s spectrum (Figure 3b) includes the dominant C–C/C–H carbons (284.98 eV) and the O–C=O carbons (288.98 eV) mainly contributed by the phospholipids, the enhanced signals of the C–N/C–O carbons (286.48 eV, strong in apoA-I) and the component N–C=O carbons (287.98 eV, unique to apoA-I) for apoA-I, and the C–S peak (285.98 eV) uniquely originate from PDP PE.[10b,12] Together with P 2p and S 2p spectra (Supporting Information, Figure S3 and S4), these data suggest that the outer lipid layer of HDL AuNPs is not composed of DPPC, but the mixture of PDP PE and DPPC that bind apoA-I.

Next, we performed an extraction with a mixture of ethanol and chloroform (1:2 in volume) to expose the underlying SAM, and then made XPS measurements (Supporting Information). With residual apoA-I (featured by the strong N 1s signal at 400.00 eV for the peptidic nitrogen and the N–C=O carbons for amide), Figure 3 show components of PDP PE: the pyridinic nitrogen at 399.00 eV for the mercaptopyridine, the dominant C–C/C–H carbons corresponding to diacyl chains and the C–S carbons in extracted HDL AuNPs. Usually, an asymmetrical disulfide tends to form a mixed SAM on the Au substrate with a mixed ratio of compositions accessible to 1:1.[10a] These data support that the underlying SAM of HDL AuNPs is a mixed SAM composed of the sulfur-containing phospholipid and 2-mercaptopyridine, two products of PDP PE reacted with Au (Figure 4).

As a good insulator, the packing of hydrocarbon chains influences the discharging of positive charges when analyzed with XPS.[13] Thus, the peak of C–C/C–H carbons provides an estimate of the packing density of acyl chains. It is notable that the C–C/C–H carbon peak (284.88 eV) in HDL AuNPs is very close to the value of 285 eV, which implies the hydrocarbon chains are well packed in the outer layer in HDL AuNPs (Figure 3b).[13] However, there is a remarkable negative shift of the C–C/C–H carbons in extracted HDL

AuNPs with a range of 0.52 eV (Figure 3b). This suggests that diacyl chains in the underlying SAM are loosely packed,[13] corresponding well to the features of SAMs on the AuNPs with high curvature around corners and edges, and mixed SAMs composed of asymmetric disulfides.[10a] To maximize hydrophobic interactions, it is energetically favorable for loosely packed hydrocarbon chains to form an interdigitated structure on the surface of nanoparticles.[14] Thus, contrary to the stacked-monolayer structure in the original model, the different arrangements of acyl chains in the outer layer and the underlying SAM suggests that the interdigitated structure is formed in the phospholipid bilayer in HDL AuNPs (Figure 4).

Next, we investigated the synergic effect between AuNPs and bound phospholipids in HDL AuNPs. PDP PE is a unique phospholipid, and different from DPPC. Its headgroup is large due to the 3-(2-pyridyldithio)propionate and carries a negative charge from the phosphate (Figure 1b). This leads to steric hindrance for PDP PE to absorb on AuNPs. With a higher curvature than that in the planar surfaces, there is increased space for PDP PE to kinetically react with the Au substrate around the corners and edges (Figure 2c). Thermodynamically, defect sites are easier for thiols or disulfides to chemisorb due to reduced activation energies.[10a] Hence, induced by the specific substrate structure of AuNP and its own specific molecular structure, PDP PE also prefers to form a mosaic SAM with high density around corners and edges in an icosahedral AuNP, and leaves the planar surfaces less covered. Notably, extracted HDL AuNPs are not stable when dispersed in chloroform although lipid monolayers can provide AuNPs miscibility to chloroform due to their lipophilicity. UV-Vis and STEM data (Supporting Information, Figure S5) imply a low surface coverage of acyl chains in the underlying SAM, which corresponds well to the feature of the mosaic SAM of PDP PE.

We further used *in-situ* DRIFTS to detect the melting phase transitions of acyl chains by measuring $\nu_s(CH_2)$ of lyophilized powders of different samples at different temperatures (Supporting Information, Figure S6 and Table 1).[15] The acyl chains in the PDP PE bilayer on AuNPs are highly disordered, starting to melt at ≤~ 25.0 °C. However, the melting of the mixed PDP PE-DPPC bilayer on AuNPs begins at ~ 35.0 °C and its T_m (the midpoint temperature of the melting process) is ~ 52.5 °C (Table 1). Further, the comparison between the lyophilized powders of PDP PE and DPPC (Table 1) illustrates that PDP PE headgroup can prevent close packing of the acyl chains and decreases hydrophobic interactions in the lamellar structure due to steric hindrance. The results suggest that the ordering of acyl chains in the phospholipid bilayer on AuNP is improved by the interposition of DPPC. DPPC tends to interpose to the planar surfaces with a low coverage of the SAM to improve the stability of the mixed PDP PE-DPPC bilayer on AuNP (Figure 1c). As such, different domains of phospholipid bilayers are formed on planar surfaces and neighboring curved faces. It is easy to form defects at borders between different domains of phospholipid bilayers formed on planar surfaces and neighboring curved faces. Correspondingly, the mixed PDP PE-DPPC bilayer on AuNPs experiences a wide ΔT (melting range) of ~ 35.0 °C (from ~ 35.0 to ~ 70.0 °C, Table 1), which supports the presence of defects. In all, the mixed PDP PE-DPPC bilayers on AuNP are featured with the mosaic interdigitated structure.

Finally, we explored the interactions between apoA-I and the mosaic phospholipid bilayers. ApoA-I has a great conformational flexibility.[6] It possesses a structural motif of the amphipathic α-helix, which are characterized by well-defined polar and non-polar faces.[6] In the lipid-free state, amphipathic α-helices fold and adopt *en face* orientation of the hydrophobic faces to form a helix bundle in the N-terminal.[6] During the lipidation process, the helix bundle gradually opens with helix–helix interactions switched to helix–lipid interactions.[6] Thus, amphipathic apoA-I can act as detergent to solubilize phospholipid bilayers and adopts continuous, fully lipidated, extended conformation (Figure 1a).[6] The ordinary phospholipid bilayer is composed of stacked monolayers, where the lipid milieu is continuous. However, PDP PE-DPPC bilayer on AuNPs is discontinuous and composed of interdigitated monolayers. Compared to the PDP PE-DPPC bilayer on AuNPs, $\boldsymbol{T_m}$ of the bilayer in HDL AuNPs is increased to ~ 57.5 °C, while $\boldsymbol{\Delta T}$ reduced to ~ 15.0 °C (from ~ 50.0 to ~ 65.0 °C, Table 1). Lipid binding to apoA-I is an exothermic process,[6b] which can improve ordering of acyl chains in the phospholipid bilayer.[3] These data suggest that apoA-I is sensitive to the defects in the PDP PE-DPPC bilayer due to the strong lipid-binding interaction. ApoA-I tends to assemble along borders between domains, close to the edges of the icosahedral AuNP, to decrease defects and improves the stability of the bilayers. As such, apoA-I is constrained from achieving a fully extended and continuous conformation (Figure 1c).

In summary, we report a mosaic interdigitated structure in the nanoparticle-templated phospholipid bilayer that supports partial lipidation of apoA-I. The structure is different from the ordinary bilayer, which is synergistically determined both by the template and the molecular structure of the bound phospholipids. The defects in the nanoparticle-templated phospholipid bilayer constrain full lipidation of apoA-I, which deviates from natural HDL formation. With decades of development, currently there are libraries of different nanoparticles and available synthetic phospholipids. Our work suggests that the nanoparticle-templated phospholipid bilayer may provide a diverse lipid milieu that takes advantage of the strong synergy between nanoparticles and bound phospholipids. As such, proteins can be modulated to diverse conformations and functions and, perhaps, rationally tailored for desired applications.

Experimental Section

Materials and chemicals

AuNPs (80 nM, 5 ± 0.75 nm, in aqueous solution) came from Ted Pella, Inc. DPPC and PDP PE were purchased from Avanti Polar Lipids, respectively. apoA-I came from Meridian Life Science, Inc. Chloroform and pure ethanol were from Sigma-Aldrich.

Synthesis of the HDL AuNPs and controls

HDL AuNPs were synthesized as reported.[7] In brief, apoA-I was added in five fold molar excess to a solution of AuNPs with a size of 5–6 nm. After 1 h, apoA-I-AuNPs were diluted by 20% by adding ethanol. PDP PE and DPPC were dissolved in ethanol to form 1 mM solutions, respectively. Each phospholipid was added to the solution of apoA-I-AuNPs in 250-fold molar excess to the AuNPs and allowed to incubate on a flat-bottom shaker for 4 h

at room temperature to form HDL AuNPs. HDL AuNPs were then purified by tangential flow filtration using a Kros Flo II tangential flow filtration system (Spectrum Labs, Inc.) fitted with #14 tubing and a 50 kDa molecular weight cutoff (MWCO)-modified polyethersulfone module to remove ethanol, free apoA-I, and phospholipids. Similarly, the AuNPs covered by mixed PDP PE-DPPC bilayers were prepared without adding apoA-I and the AuNPs covered by PDP PE bilayers were formed without adding both apoA-I and DPPC.

Extraction of the outer layer of HDL AuNPs

Mixtures of alcohol and chloroform solvents are frequently used to extract lipids from biological samples.[16] To further measure the underlying lipid SAMs, we employed a mixture of ethanol and chloroform (1:2 in volume) to remove the outer layer of phospholipids. 0.5 mL HDL AuNP (2 μM, in aqueous solution) was mixed with 15 mL ethanol-chloroform and allowed to incubate overnight at room temperature. The solution was then sonicated for 30 minutes. Then, the solution was centrifuged (15,000 RPM × 10 mins at 5 °C) to pellet the nanoparticles and to remove the supernatant containing extracted lipids. This procedure was repeated (× 3) using pure ethanol to rinse the nanoparticles. The treated precipitates were then dispersed in chloroform under sonication, and the "extracted HDL AuNPs" were used for further measurements.

Characterization of HDL AuNPs and controls

TEM and HRTEM images of bare AuNPs were taken on a JEOL JEM-2100F Transmission Electron Microscope at 200 kV. Prior to imaging, bare AuNPs were deposited on carbon-coated copper TEM grids (CF300-Cu, Electron Microscopy Sciences), which were then dried using filter paper.

To prepare samples for XPS experiments, concentrated dispersions of HDL AuNPs and extracted HDL AuNPs, and solutions of different controls were deposited on silicon wafers and dried under vacuum overnight. XPS spectra were acquired with a Thermo Scientific Escalab 250Xi photoelectron spectrometer using a monochromatic Al-K_α X-ray source (1486.6 eV) and the vacuum in the analysis chamber was maintained at 10^{-9} mbar or lower. X-ray power, pass energy of the analyzer, and takeoff angle of the photoelectron were set at 150W, 20 eV, and 90°, respectively. The energy resolution of this system is less than 0.42 eV, estimated by the Ag $3d_{5/2}$ peak width at our measurement condition. The binding energy obtained from the XPS spectra of different AuNPs was calibrated using the Au $4f_{7/2}$ peak (84.0 eV), while those of DPPC, PDP PE and apoA-I were calibrated by the C 1s peak of C–C and C–H carbons (285.0 eV). The curves were fitted with the NLLSF (non-linear least squares fitting) method using Avantage software, version 5.51.

UV-Vis absorbance spectra of different AuNPs and the concentration of HDL AuNPs were obtained using an Agilent 8453 UV-Vis spectrophotometer (Agilent Technologies), as reported.[7]

STEM was performed on a HD-2300A microscope operating at 200 kV (Hitachi) to get the high-angle annular dark-field (HAADF) images of extracted HDL AuNPs. Prior to imaging with STEM, different AuNPs dispersed in water or chloroform were deposited on carbon-

coated copper TEM grids (CF300-Cu, Electron Microscopy Sciences) respectively, which were then dried using filter paper.

The DRIFTS of lyophilized powders of HDL AuNPs, AuNPs covered by different lipid bilayers and the controls were measured on a Nicolet 6700 FTIR spectrometer (Thermo Scientific) equipped with an MCT detector and a Harrick praying mantis accessory. To get lyophilized powders, concentrated dispersions of HDL AuNPs and AuNPs covered by different lipid bilayers were frozen by liquid nitrogen and lyophilized with a FreeZone 6 Liter Cascade Console Freeze Dry System for 24 hours, respectively. Approximately 10 mg of each sample mixed with KBr powder was loaded into the *in situ* environmental cell (Harrick, Praying Mantis™). After the background collection of KBr powder, all spectra were collected with a resolution of 4 cm^{-1} over 32 scans under an Argon atmosphere (UHP, at a flow rate of 120 sccm) at designed temperatures (gradually increased by a step of 5 °C from 25 °C).

Supplementary Material

Refer to Web version on PubMed Central for supplementary material.

Acknowledgments

This work made use of the Keck-II facility and EPIC facility of the NUANCE Center at Northwestern University, which has re-ceived support from the MRSEC program (NSF DMR-1121262) at the Materials Research Center; the International Institute for Nano-technology (IIN); the Keck Foundation; and the State of Illinois, through the IIN. We thank Dr. Xinqi Chen and Dr. Jingsong Wu for technical assistance. We thank the Howard Hughes Medical Institute (HHMI) for a Physician Scientist Early Career Award, the Department of Defense/Air Force Office of Scientific Research (FA95501310192 and FA9550-11-1-0275), the National Institutes of Health/National Cancer Institute (U54CA151880 and R01CA167041), and the Science and Technology Project (Major Program) of Hubei Provincial Education Department, China (Grant No. z20081401). This material is based on research sponsored by the Air Force Research laboratory under agreement number is FA8650-15-2-5518. The U.S. Government is authorized to reproduce and distribute reprints for Governmental purposes notwithstanding any copyright notation thereon. The views and conclusions contained herein are those of the authors and should not be interpreted as necessarily representing the official policies or endorsements, either expressed or implied, of Air Force Research Laboratory or the U.S. Government.

References

1. a) Israelachvili, Marcelja S, Horn RGQ. Rev. Biophys. 1980; 13:121.b) Hauser H, Pascher I, Pearson RH, Sundell S. Biochim. Biophys. Acta. 1981; 650:21. [PubMed: 7020761]
2. a) Bretscher MS. Science. 1973; 181:622. [PubMed: 4724478] b) Edidin M. Nat. Rev. Mol. Cell Biol. 2003; 4:414. [PubMed: 12728275]
3. a) Shaw AW, McLean MA, Sligar SG. FEBS. Lett. 2004; 556:260. [PubMed: 14706860] b) Nath A, Atkins WM, Sligar SG. Biochem. 2007; 46(8):2059. [PubMed: 17263563]
4. a) Lee YK, Lee H, Nam J-M. NPG Asia Mater. 2013; 5:e48.b) Tan S, Li X, Guo Y, Zhang Z. Nanoscale. 2013; 5:860. [PubMed: 23292080] c) Mashaghi S, Jadidi T, Koenderink G, Mashaghi A. Int. J. Mol. Sci. 2013; 14:4242. [PubMed: 23429269]
5. Mu Q, Jiang G, Chen L, Zhou H, Fourches D, Tropsha A, Yan B. Chem. Rev. 2014; 114(15):7740. [PubMed: 24927254]
6. a) Phillips MC. J. Lipid. Res. 2013; 54:2043.b) Phillips MC. J. Biol. Chem. 2014; 289:24020. [PubMed: 25074931]
7. a) Thaxton CS, Daniel WL, Giljohann DA, Thomas AD, Mirkin CA. J. Am. Chem. Soc. 2009; 131(4):1384. [PubMed: 19133723] b) Luthi AJ, Zhang H, Kim D, Giljohann DA, Mirkin CA, Thaxton CS. ACS Nano. 2011; 6(1):276. [PubMed: 22117189] c) McMahon KM, Mutharasan RK,

Tripathy S, Veliceasa D, Bobeica M, Shumaker DK, Luthi AJ, Helfand BT, Ardehali H, Mirkin CA, Volpert O, Thaxton CS. Nano Lett. 2011; 11(3):1208. [PubMed: 21319839] d) Luthi AJ, Lyssenko NN, Quach D, McMahon KM, Millar JS, Vickers KC, Rader DJ, Phillips MC, Mirkin CA, Thaxton CS. J. Lipid Res. 2015; 56(5):972. [PubMed: 25652088] e) Yang S, Damiano MG, Zhang H, Tripathy S, Luthi AJ, Rink JS, Ugolkov AV, Singh AT, Dave SS, Gordon LI, Thaxton CS. Proc. Natl. Acad. Sci. U.S.A. 2013; 110(7):2511. [PubMed: 23345442] f) Plebanek MP, Mutharasan RK, Volpert O, Matov A, Gatlin J, Thaxton CS. Sci. Rep. 2015; 5:15724. [PubMed: 26511855]

8. a) Hofmeister H. Encyclopedia of nanoscience and nanotechnology. 2004; 3:431.b) Niu W, Xu G. Nano Today. 2011; 6(3):265.c) Sun Y, An C. Front. Mater. Sci. 2011; 5(1):1.
9. Zhang Q, Xie J, Yang J, Lee JY. Acs Nano. 2008; 3(1):139.
10. a) Love JC, Estroff LA, Kriebel JK, Nuzzo RG, Whitesides GM. Chem. Rev. 2005; 105(4):1103. [PubMed: 15826011] b) Sun W, Kewalramani S, Hujsak K, Zhang H, Bedzyk MJ, Dravid P, Thaxton CS. Langmuir. 2015; 31(10):3232. [PubMed: 25695627]
11. Jansen R, Van Bekkum H. Carbon. 1995; 33(8):1021.
12. McArthur, SL., Mishra, G., Easton, CD. Surface Analysis and Techniques in Biology. Smentkowski, VS., editor. Vol. Ch. 2. Switzerland: Springer; 2014.
13. a) Duwez A-S. J. Electron Spectrosc. Relat. Phenom. 2004; 134:97.b) Zharnikov M, Grunze M. J. Phys.: Condens. Matter. 2001; 13:11333.
14. a) Fan H, Yang K, Boye DM, Sigmon T, Malloy KJ, Xu H, López GP, Brinker CJ. Science. 2004; 304:567. [PubMed: 15105495] b) Patil V, Mayya KS, Pradhan SD, Sastry M. J. Am. Chem. Soc. 1997; 119:9281.c) Ahmed S, Wunder SL. Langmuir. 2009; 25(6):3682. [PubMed: 19231878]
15. a) Lewis RNAH, McElhaney RN. Biochim. Biophys. Acta, Biomembr. 2013; 1828:2347.b) Griffiths, PR., De Haseth, JA. Fourier transform infrared spectrometry. USA: John Wiley & Sons; 2007.
16. a) Bligh EG, Dyer WJ. Can. J. Biochem. Physiol. 1959; 37:911. [PubMed: 13671378] Wang W, Gustafson A. J. Lipid Res. 1994; 35:2143. [PubMed: 7897312] Ito, J-i, Nagayasu, Y., Kato, K., Sato, R., Yokoyama, S. J. Biol. Chem. 2002; 277:7929. [PubMed: 11773045]

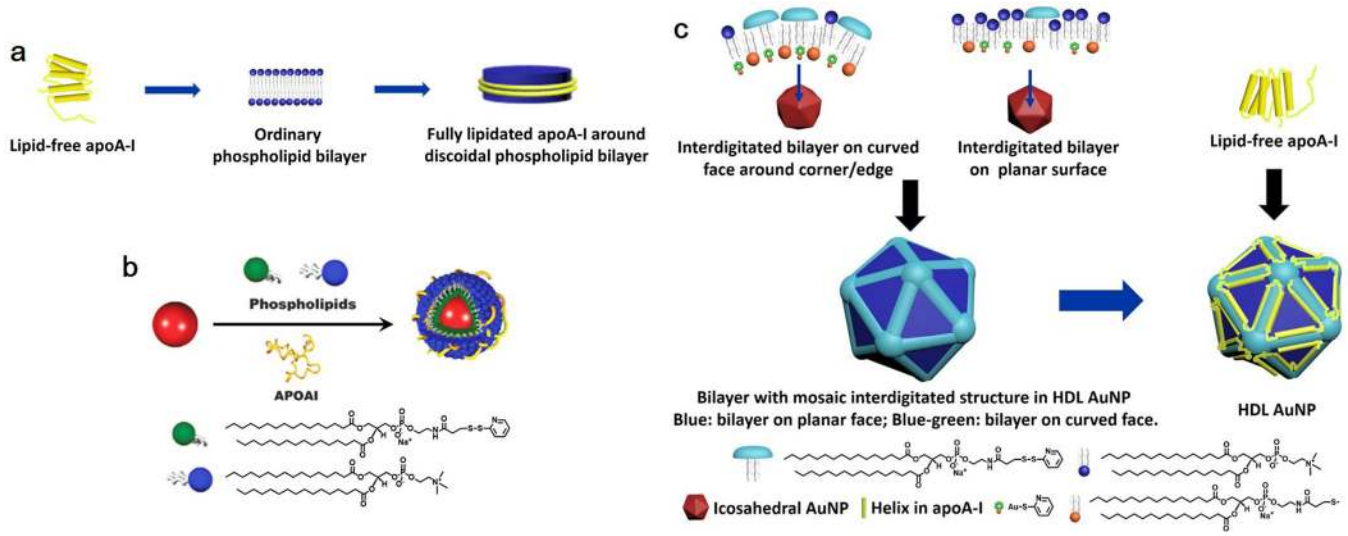

Figure 1.

Full lipidation of apoA-I with the ordinary phospholipid bilayer (a). The original (b) and revised (c) models of HDL AuNP.

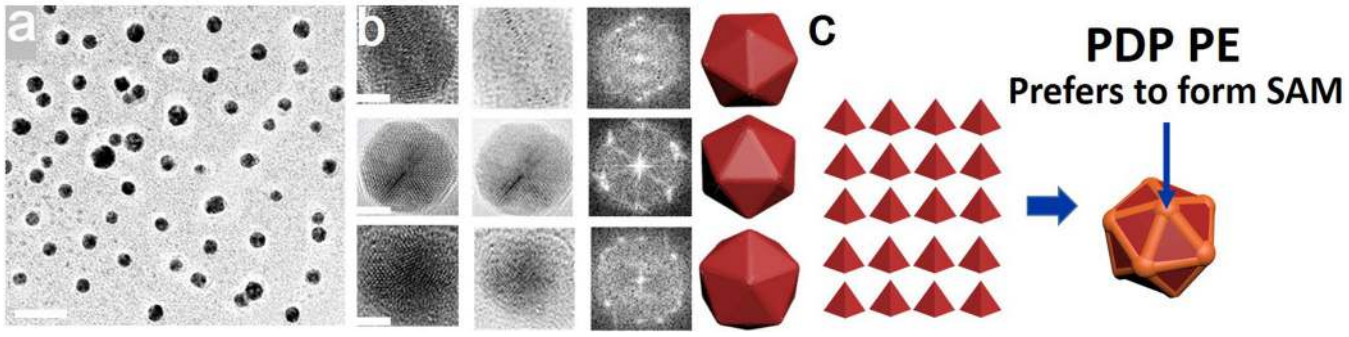

Figure 2.

(a) TEM image of icosahedral Au NPs (the scale bar: 20 nm). (b) HRTEM "fingerprints" of icosahedral Au NPs (the scale bar, 2nm) in various orientations : "edge" (along the two-fold symmetry axis), "face" (along the three-fold symmetry axis) and "fivefold" (along the three-fold symmetry axis) from top to bottom, together with corresponding noise-reduced images (generated by inverse fast Fourier trans-formation (FFT) procedures), diffractograms (generated by conventional two-dimensional FFT) and models from left to right in each row. (c) Mosaic surface of an Au NP, where PDP PE prefers to form SAM around corners and edges.

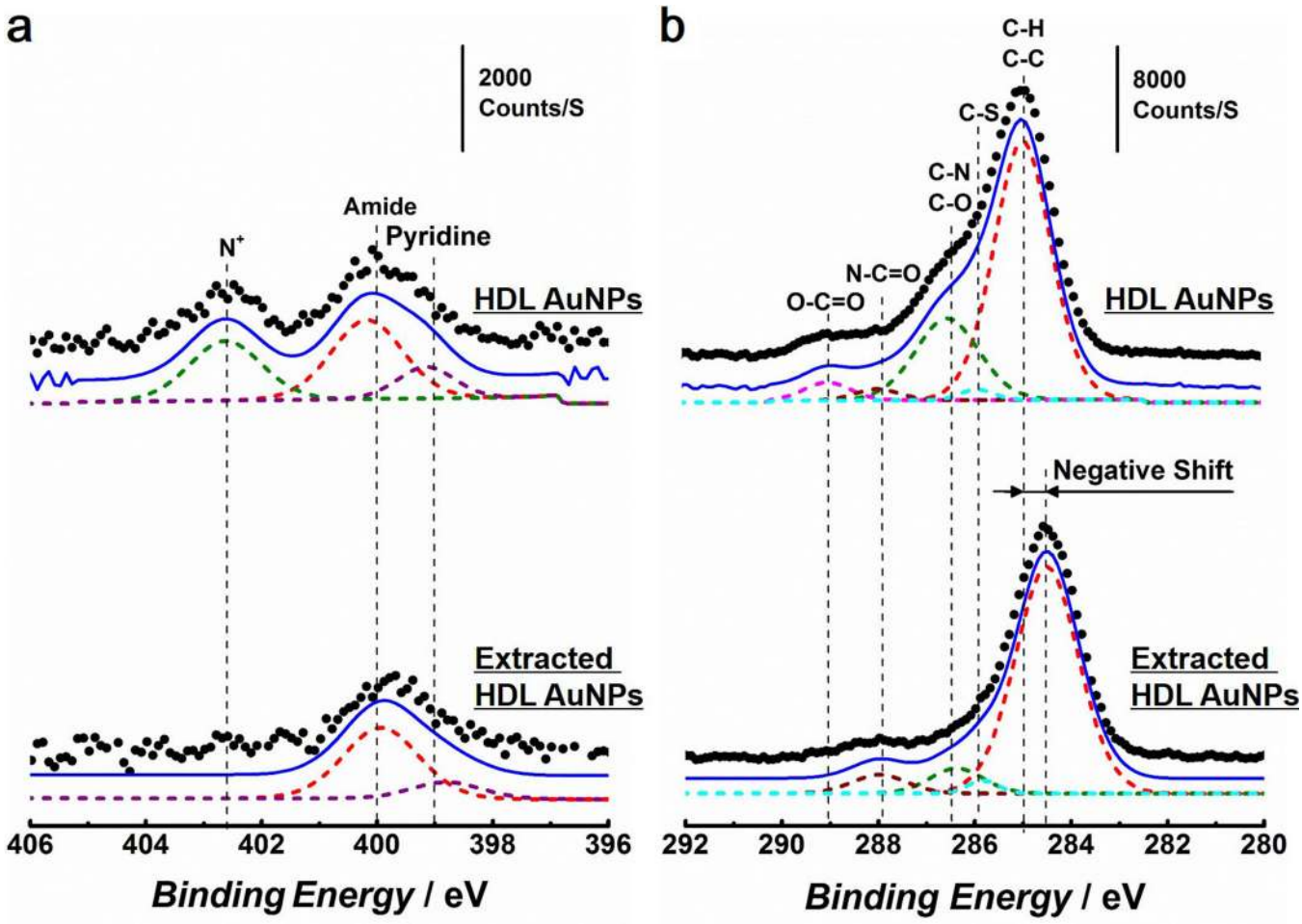

Figure 3.

XP spectra of HDL AuNPs and extracted HDL AuNPs: N 1s region (a) and C 1s region (b). In each spectrum, the experimental data (black dots) are compared to a simulated spectrum (blue solid-line), which is subdivided into chemically shifted components (short dash-lines).

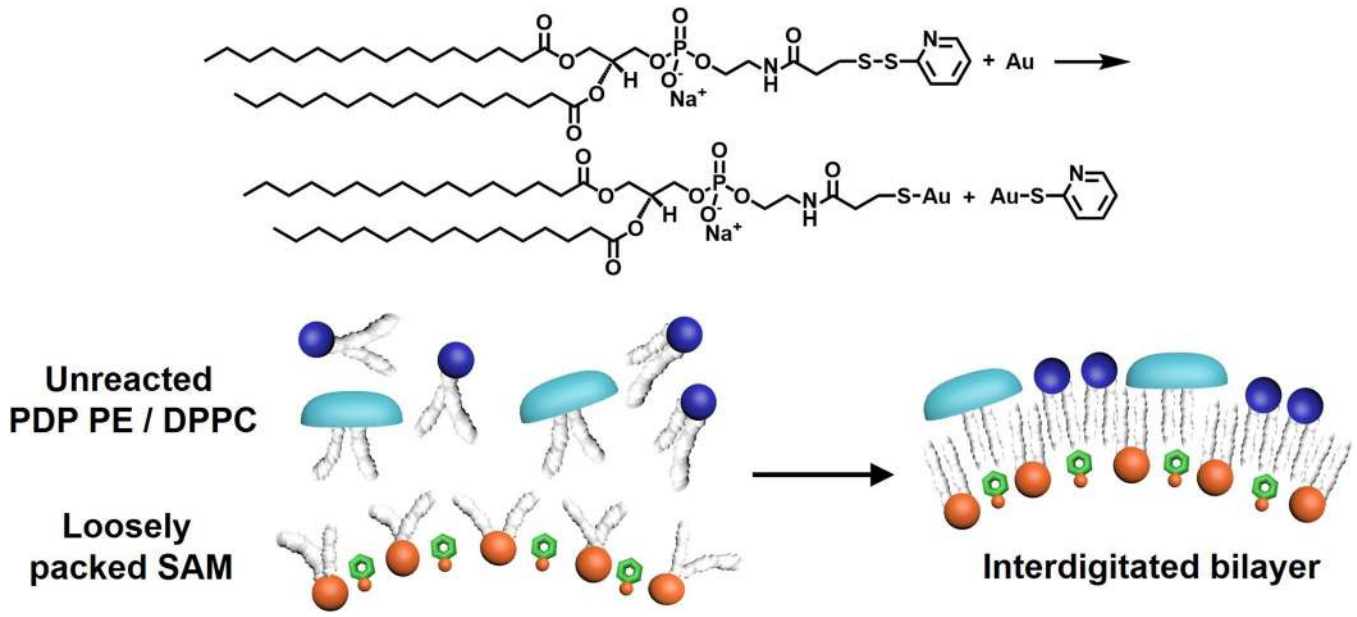

Figure 4.
Reaction between PDP PE and Au, and formation of the interdigitated bilayer.

Table 1

Acyl chain-melting process monitored by in-situ DRIFTS

Lyophilized Powder	T_m (°C) *a)*	ΔT (°C) *b)*
PDP PE	~ 45.0	~ 40.0 – ~ 50.0
DPPC	~ 97.5	~ 95.0 – ~ 100.0
AuNPs with PDP PE bilayer		Melting process takes place at ≤~ 25.0 °C
AuNPs with mixed PDP PE-DPPC bilayer	~ 52.5	~ 35.0 – ~ 70.0
HDL AuNPs	~ 57.5	~ 50.0 – ~ 65.0

a) T_m: the midpoint temperature of the melting process;

b) ΔT: the melting range.